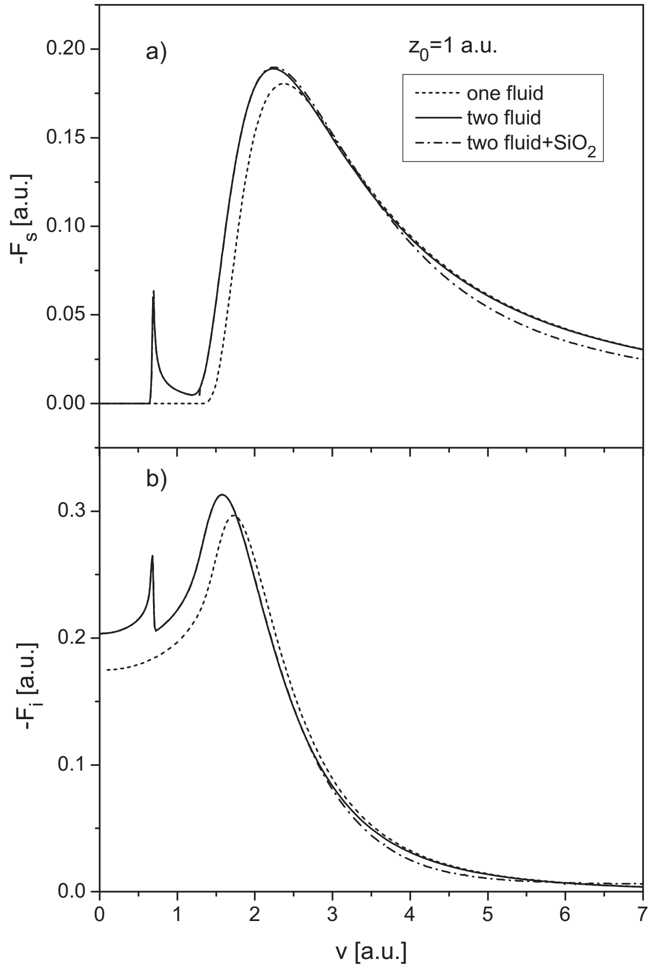

FIG. 1. The dependencies on speed v (in a.u.) of (a) stopping and (b) image forces (in a.u.) on proton moving at distance $z_0 = 1$ a.u. above graphene in the cases: (solid lines) two-fluid model without substrate, (dashed lines) one-fluid model without substrate, (dash-dotted lines) two-fluid model with SiO_2 substrate (with $\epsilon \approx 3.9$ and $h \approx 4.2$ a.u.).

that the screening ability of graphene is diminished at high frequencies [cf. Eqs. (10) and (11)], so that the image force on the projectile is then simply reduced to the static screening by the substrate.

Figures 1 and 2 also imply a strong decrease in the magnitudes of both the stopping and image forces with increasing distances of proton from graphene, which is further illustrated in Fig. 3 for the two-fluid model without a substrate and for three speeds: $v=1$, 3, and 5. The effects of the substrate are so weak in this parameter range that we only show in Fig. 3 the curves corresponding to speed $v=5$ for the case of graphene above the SiO_2 substrate, described as in Figs. 1 and 2. One notices in Fig. 3 that the decay rates of both stopping and image forces are strongly affected by the proton speed, in accordance with the results found for carbon nanotubes [26,29,36].

For a point dipole moving along the x axis with speed v at the distance $z_0 > 0$ above graphene, we shall use the angles from spherical coordinates to describe the orientation of its moment, $\boldsymbol{\mu} = \{\mu_x, \mu_y, \mu_z\} \equiv \mu\{\sin\theta\cos\varphi, \sin\theta\sin\varphi, \cos\theta\}$,

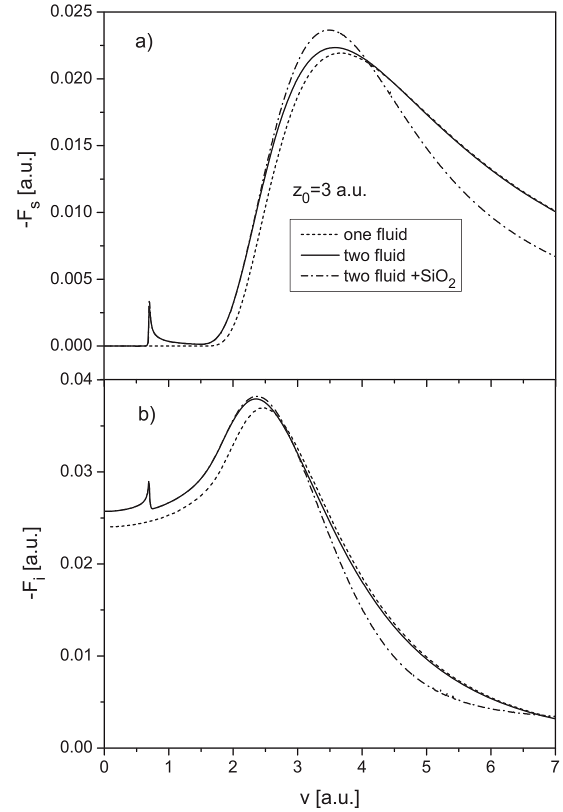

FIG. 2. The dependencies on speed v (in a.u.) of (a) stopping and (b) image forces (in a.u.) on proton moving at distance $z_0 = 3$ a.u. above graphene in the cases: (solid lines) two-fluid model without substrate, (dashed lines) one-fluid model without substrate, (dash-dotted lines) two-fluid model with SiO_2 substrate (with $\epsilon \approx 3.9$ and $h \approx 4.2$ a.u.).

with the polar angle θ taken relative to the z axis and the azimuthal angle φ relative to the direction of motion, i.e., the x axis. So, the stopping and the image forces on the dipole are, respectively,

$$F_s^{(d)} = \frac{\mu^2}{2\pi}\int\int dk_x dk_y e^{-2kz_0}\frac{k_x}{k}[(k_x\cos\varphi + k_y\sin\varphi)^2\sin^2\theta + k^2\cos^2\theta]\mathrm{Im}\left[\frac{1}{D(k,k_x v)}\right], \tag{29}$$

$$F_i^{(d)} = \frac{\mu^2}{2\pi}\int\int dk_x dk_y e^{-2kz_0}[(k_x\cos\varphi + k_y\sin\varphi)^2\sin^2\theta + k^2\cos^2\theta]\mathrm{Re}\left[\frac{1}{D(k,k_x v)} - 1\right]. \tag{30}$$

In Figs. 4 and 5 we consider the case of a point dipole at distance $z_0=3$ having the moment of magnitude $\mu=1$, which is oriented in the xz plane (that is, $\varphi=0$) with its direction relative to the z axis given by the angle θ. Figure 4 shows the velocity dependencies of the stopping and image forces for three orientations: $\theta=0$, 45°, and 90° shown with solid, dashed and dash-dotted lines, respectively, whereas Fig. 5 shows the full dependencies on both the angle θ and speed v.